International Journal of Multiphase Flow 53 (2013) 65–74

Contents lists available at SciVerse ScienceDirect

International Journal of Multiphase Flow

journal homepage: www.elsevier.com/locate/ijmulflow

Experimental study on the performance of a novel structure for two-phase flow distribution in parallel vertical channels

P. Yuan [a], G.B. Jiang [a], Y.L. He [a], X.L. Yi [b], W.Q. Tao [a,*]

[a] Key Laboratory of Thermo-Fluid Science and Engineering of MOE, School of Energy and Power Engineering, Xi'an Jiaotong University, Xi'an 710049, Shaanxi, China
[b] Sichuan Air Separation Plant (Group) Company, Jianyang 641400, Sichuan, China

ARTICLE INFO

Article history:
Received 7 March 2012
Received in revised form 19 May 2012
Accepted 22 May 2012
Available online 21 June 2012

Keywords:
Distributor
Plate-fin heat exchanger
Multiphase flow
Parallel channels

ABSTRACT

Uniform flow distribution is critical to obtain high thermal performance in many heat and mass transfer devices. It especially plays an important role in a compact heat exchanger. In this paper, a two-phase flow distributor is proposed for the evaporator unit of the plate-fin heat exchanger to alleviate the phase maldistribution in the multiphase flow. Air and water mixture was adopted as two-phase medium and distributions into ten parallel channels were measured in detail. The results show that the proposed distributor can improve the two-phase flow distribution of the plate-fin heat exchanger.

1. Introduction

Plate-fin heat exchangers are characterized by the small temperature differences between two heat transfer fluids, the high thermal effectiveness, the large heat transfer area per unit volume, the low weight per unit heat transfer rate, and possibility of heat exchange between many process streams. Due to these excellent characters the plate-fin heat exchangers are widely used in many industrial fields, such as chemical engineering, petroleum refining, and food processing. In the plate-fin heat exchanger, in order to embody a large heat transfer surface in a small volume a lot of small parallel channels are used for making the effective use of the available primary and secondary surfaces. It is essential to uniformly distribute the streams among all parallel channels for required thermal performance. However, to distribute the stream uniformly among the parallel channels is difficult to be implemented and maldistribution often occurs in the plate-fin heat exchanger.

In order to improve the flow distribution among parallel channels in the units of the plate-fin heat exchangers, many studies have been performed so far. A brief review on this topic is presented below. Mueller and Chiou (1988) pointed out in their review paper that a non-uniform flow distribution in channels leads to different performance penalties depending on the flow process, and the gross flow maldistribution leads to a significant reduction in effectiveness for high NTU heat exchangers. Lalot et al. (1999) studied the fluid distribution in different heat exchangers, and their results showed that the gross flow maldistribution leads to an efficiency loss of about 7% for condensers and counter flow heat exchangers, and up to 25% for cross flow exchangers. The two-phase flow structure in the compact heat exchanger is very complex, and two-phase flow maldistribution is most likely to occur. In the following attention is turned on the studies of the maldistribution of two-phase flow.

In order to improve the two-phase flow distribution, usually some special structures, say manifold, T-junction or specially-designed distributors, are adopted. Kitto and Robertson (1989) pointed out that parameters influencing the two-phase flow maldistribution are numerous, such as geometric factors (manifold cross-section dimensions, branch couplings, location and orientation of the tubes) and operating factors (flow rate, flow patterns, vapor fraction at the inlet of the manifold and heat load on the tubes). Bernoux et al. (2001) made an experiment, simulating the two-phase flow distribution at the inlet manifold of compact heat exchangers by refrigerant R113. They found that the vapor distribution in each channel became uniform with the increase of mass flux, but the liquid distribution still remained unbalanced, and the liquid distribution through the channels was not much sensitive to the mass flux. Their research showed that different mass flow ratio of two fluids lead to different gas and liquid distribution. Vist and Pettersen (2004) investigated the two-phase flow distribution in the manifold with refrigerant R134a. Their results showed that two-phase flow distribution is little affected by the change of the heat load of the evaporator, but two-phase flow distribution has the great influence on the heat transfer. Several authors (Lahey,

* Corresponding author. Tel./fax: +86 29 82669106.
E-mail address: wqtao@mail.xjtu.edu.cn (W.Q. Tao).

0301-9322/$ - see front matter © 2012 Elsevier Ltd. All rights reserved.
http://dx.doi.org/10.1016/j.ijmultiphaseflow.2012.05.006

1986; Osakabe et al., 1999; Seeger et al., 1986) investigated two-phase flow distribution in T-junctions with several outlets, concluding that T-junctions cannot be directly applied to improve the flow distribution. Tondeur and Luo (2004) designed a new type of distributor called "constructual distributor" which was composed of multiscale internal channel networks and was optimized on the basis of a compromise between certain constraints (such as minimal viscous dissipation and void volume). This structure is expected to give uniform flow distribution. However, their preliminary experimental validation still showed 20% flow rate difference. They attributed this essentially to the manufacture imperfection. Based on a quite general theory of multiscale shapes and structures in nature and engineering fields developed by Bejan (1997, 2000), Bejan and Tondeur (1998), Yue et al. (2010) designed a constructural distributor for multi-microchannels, and conducted experimental and numerical studies. They got a good uniform stream distribution at the high gas flow rate. Osakabe et al. (1999) conducted experimental study of air–water distribution for a manifold with four outlets. It was found that a larger length of the outlet tube can improve the distribution of single phase flow but deteriorate the distribution for two-phase bubble flow. Kim and Han (2008) investigated the effect of protrusion depth of the outlet tube of a manifold on the distribution of air–water mixture. It is found that with the increase in the protrusion depth the flow maldistribution increases. Webb and Chung (2005) investigated the two-phase flow distribution phenomena in multiple header-tube junctions used in heat exchangers, and found that the flow distribution is strongly influenced by the header orientation (horizontal or vertical), the number of branch tubes, the flow direction in the header (up flow or down flow), the header shape and tube end projection into the header, and the location and orientation of the inlet and exit connections. They concluded that the design of devices to improve flow distribution is "highly empirical". Jiao and Baek (2005) proposed a concept of the evaporator design by adding a complementary fluid cavity in the distributor, and their experiment results showed that the most suitable distributor parameter, which contains the width of the complementary fluid cavity, is about 0.22. Ha et al. (2006) carried out numerical studies for air–water two-phase flow distributions in multi-channels between two headers. It was found that with the increase in liquid flow rate the flow distribution uniformity becomes worse. The flow distribution in a short header for different flow orientations and flow patterns to the parallels pipes were experimentally investigated by Ahmad et al. (2009), and their results showed that the most severe maldistribution occurs for the vertical upward channel configuration. Marchitto et al. (2009) investigated flow maldistribution in parallel channels by a series of fittings able to affect the flow distribution along downstream of the head. Among the fitting devices used, the insertion of a co-axial, multi-hole distributor inside the header confirms the possibility of greatly improving the liquid and gas flow distribution by the proper selection of position and diameter. In addition, the references (Marchitto et al., 2008; Wen and Li, 2004; Yuan, 2003; Zhang and Li, 2003) conducted some similar researches.

One can conclude from the above reviews that although a great number of investigations on this topic have been carried out, a generally applicable method (not to say a perfect method) to realize the uniform distribution of the gas and liquid two-phase flow is still not obtained yet so far. Therefore it is necessary and crucial to perform further study in this regard.

It must be pointed that the maldistribution of the gas and liquid phases in compact heat exchangers, such as the plate-fin heat exchangers, is more evident in contrast with other types of heat exchangers, which results in the fact that compact heat exchangers cannot be applied to improve the heat transfer efficiency of the gas and liquid two-phase flow if this disadvantage cannot be efficiently overcome. The major purpose of the present study is to conduct an experimental investigation for the proposed configuration of the two-phase flow distributor and to reveal its basic performance.

2. Experiment setup and measurement system

2.1. Outline of the new distributor

A typical structure of the plate fin heat exchanger is shown in Fig. 1a. The major character of this structure is that gas and liquid simultaneously flow into the header and then flow along some parallel channels as shown in Fig. 1b. These parallel channels serve as stream guidance devices and are called flow fence. The purpose of the flow fence in the head is to guide the flow stream to the parallel channels in every unit of the plate fin heat exchanger. However, when the flow direction changes in the flow fence because of the fence shape, phase separation often occurs under the influence of the inertia force due to the density difference, ie. inertia difference, between the gas and liquid, maldistribution may be caused seriously in the downstream small parallel passages. In the present

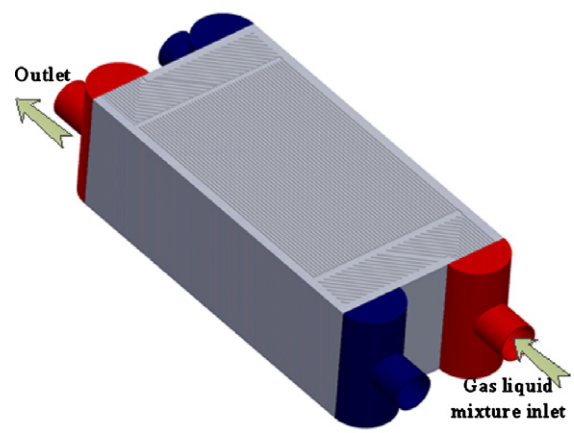

(a) Typical plate-fin heat exchanger

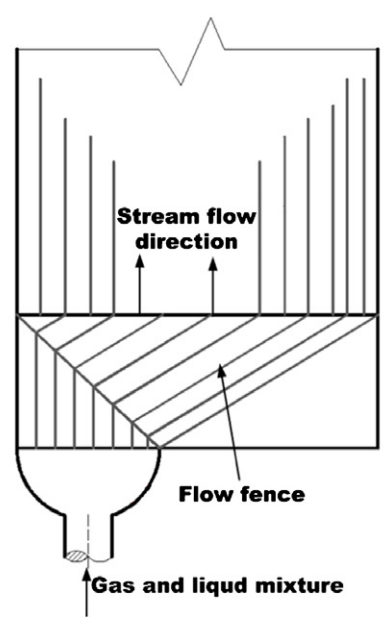

(b) Interior structure of flow distribution

Fig. 1. Typical plate-fin heat exchanger and flow distribution structure.

study a novel flow inlet structure is proposed, in which the gas and liquid phases enter into the plate-fin heat exchange separately and a specially-designed distributor is provided to mix the two phases and distribute the mixture more uniformly in the subsequent parallel channels.

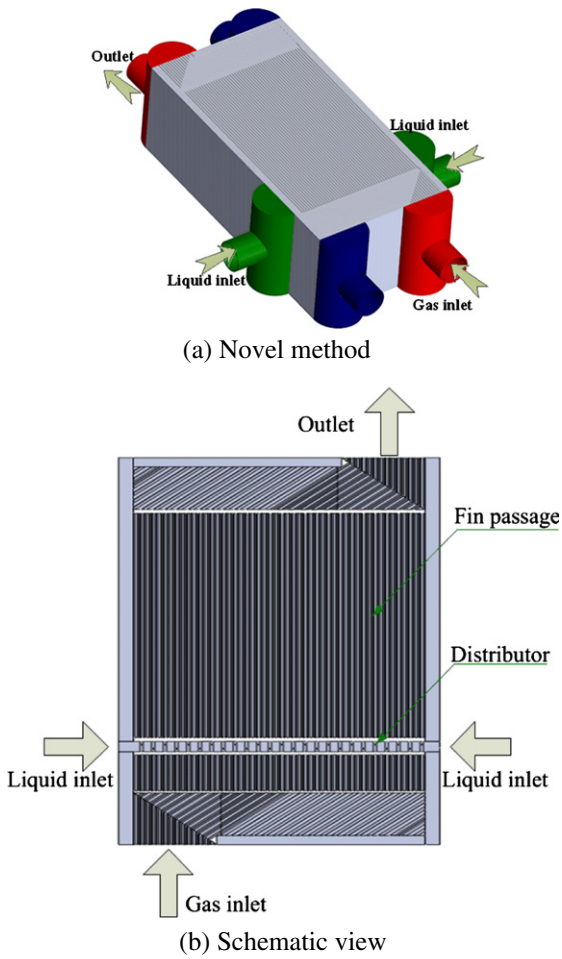

Fig. 2. A novel structure for flow distribution.

The above arrangement for the two-phase flow inlet implies that the two-phase mixture should be separated into single gas and liquid phase before entering into the inlet, and the gas and liquid phase are transported into the heat exchanger through their respective routes. The arrangement of gas phase and liquid phase inlets is shown in Fig. 2a and the interior structure is schematically presented in Fig. 2b. It should be noted that illustrated in Fig. 2 is only the structure for one unit. A plate-fin heat exchanger is usually consisted of many units and the same structure is adopted in each unit. This differs from the conventional structure as shown in Fig. 1, where the two-phase mixture in the head is supplied to all units in the heat exchanger.

The major purpose of the present study is to experimentally investigate the distribution performance for one structure of such novel distributor via air–water two-phase mixture and examine the major influencing factors. In the following the experimental setup will first be introduced, followed by a description of the tested flow distributor. Then air–water mixture distribution test procedure will be presented, followed by the analysis and discussion of the test data. Finally some conclusions will be made.

2.2. Experiment setup

The experimental system is schematically shown in Fig. 3. Air and water were used as the test fluids. The system comprises of two supply lines, where water and air are carried into the water inlets and air inlets of the test section separately. The gas and liquid phase mix each other in the gas liquid distributor, and then the mixture stream is distributed into subsequent 10 parallel channels. Air and water mixture flow downstream through the 10 parallel channels, then reach the 10 separators for phases measurements. The water flow rate was measured by reading the height of the water accumulation within a certain period of time. The air flow rate was measured by the volume flow meter for each channel.

Fig. 4 provides the detail of the test section, the core of which is a specially designed distributor. The test section is vertically arranged with three parts: the bottom part is the gas supply part,

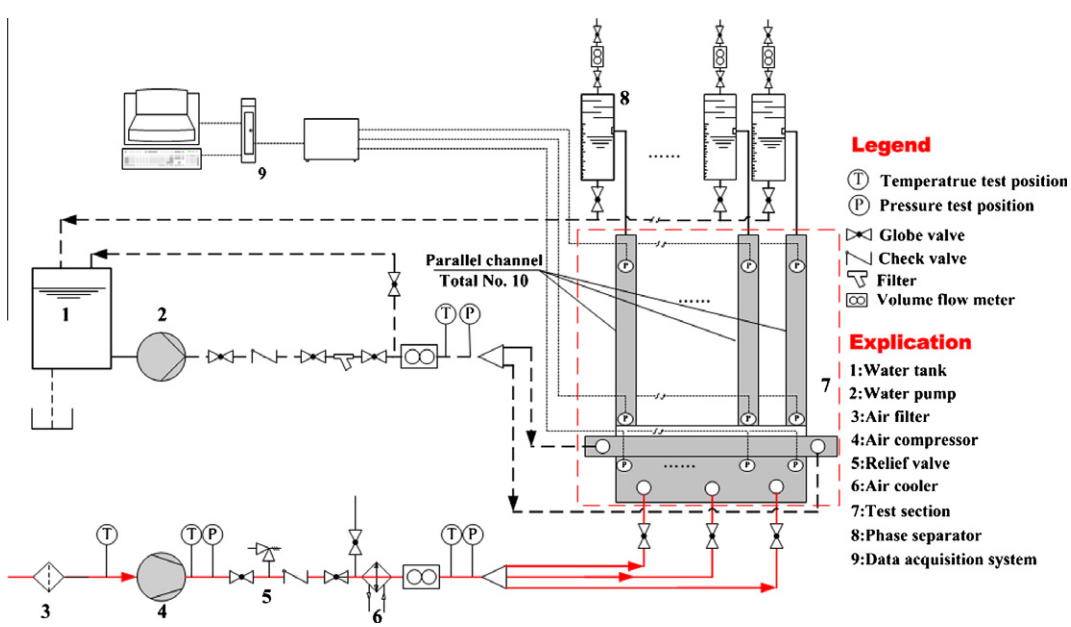

Fig. 3. Scheme of the test apparatus.

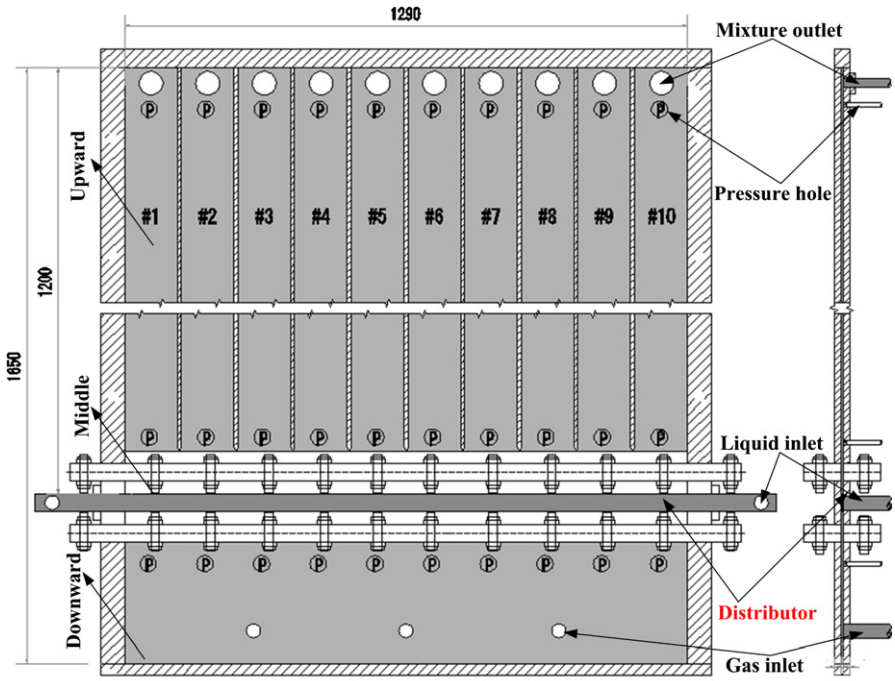

(a) Schematic of test section and position of pressure-taps

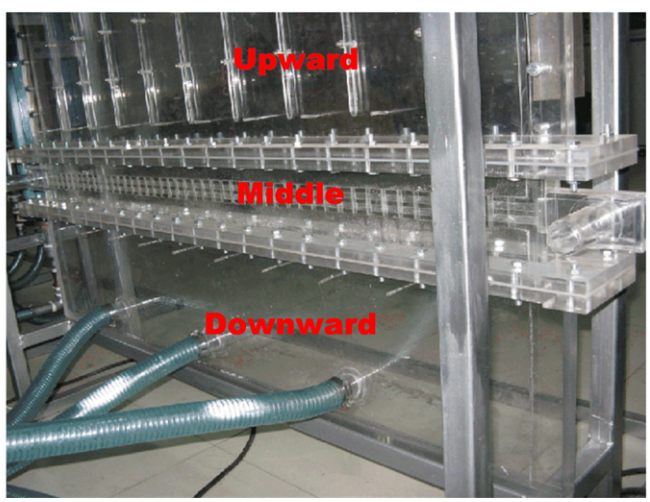

(b) Photo of test section

Fig. 4. Detail of test section.

the middle part is the gas liquid distributor and the top part is parallel channels. In engineering practice the number of the parallel channel is numerous. In order to simulate the distribution character of the tested distributor when used for the subsequent vast parallel channels in real practice and not to make the experimental measurement too complicated, the vast parallel channels are simplified by 10 channels with equal cross section. The three parts of the test section are designed in such a way that all can be observed visually. Also shown in Fig. 4a are the approximate position of the pressure taps for each sub-channel.

Fig. 4b exhibits the photo of the test section. There are 20 pressure tap lines in the downward and upward of the distributor to record the pressure of the tested distributor, and another 10 pressure taps are installed at 10 mixture outlets. The surface plate thickness of the bottom and top part is 15 mm to bear the pressure of flows. The bottom, middle and top parts are joined into the whole one by the structure of flanges and gaskets.

A picture and the details of the distributor structure are shown in Fig. 5, whose three outline dimensions are 1290, 40 and 6.5 mm for the length, width and height, respectively. As shown in Fig. 5 the distributor consists of gas channels, liquid channels and connects columns. Two liquid inlets are arranged at the two sides of the distributor with a diameter of 25 mm for water to enter the liquid channels. The gas phase flows into the vertical gas passages of the distributor from the gas inlet, the liquid phase flows into the crosswise liquid passages of the distributor from the liquid inlets, and the gas and liquid channels are connected through the cylindrical passages (hole). The liquid phase sprays into the gas channels from the liquid passages through the cylindrical holes, finishing primarily mixing with the gas phase from the vertical gas passages. Then the two-phase mixture enters into downstream ten parallel channels.

The three gas inlets ahead of the test section are directly connected to the total gas pipe, where manometer and temperature

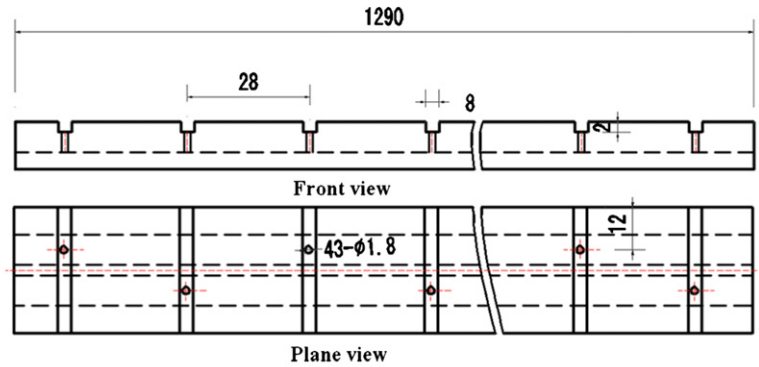

(a) Views of the distributor

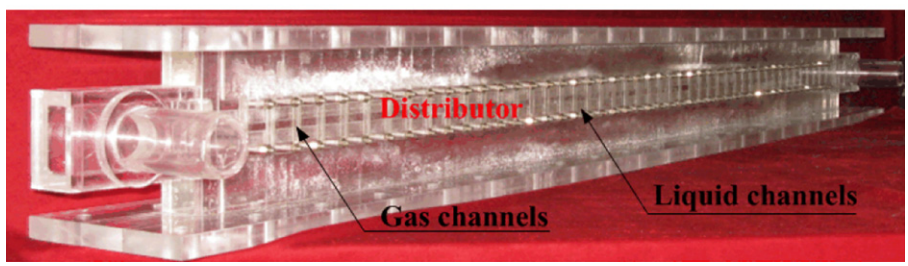

(b) Photo of the distributor

Fig. 5. Detail of the distributor.

gauge are installed immediately before the gas inlets to monitor the total pressure and temperature of the gas before entering into the test section. Water are delivered to the test distributor by a water pump, water manometer and flow meter are installed in the total water pipe to record the total pressure and volume flow rate. The total water pipe is divided into 2 equal manifolds to deliver the water to both water inlets, which lie in the both sides of the distributor (Fig. 5).

The 10 gas and liquid separators (Fig. 6) receive the mixture coming from the 10 parallel channel. The separators are a cubic geometry and made of transparent glass. Fences are arranged at the upper part to separate gas and liquid phase. The gas phase passes through the fence and reaches to the gas flow meters, then released into the atmosphere. The liquid stops and falls into the bottom of the separator.

2.3. Measurement system

There are three operation parameters for this study: temperature, pressure and flow rate. They are measured by following methods.

2.3.1. Volume flow rate

For the gas rota-meters with a range of 1.67E−03–1.67E−02 $m^3\,s^{-1}$ are used to measure the volume flow rate. For water, ten square-cross-sectional cylindrical containers (i.e. phase separators) are used to measure the liquid volume flow rate of each channel. The dimensions of the cylinder are 300 (length) × 300 (width) × 550 mm (height). The liquid phase flow rate can be calculated by the measuring the height variation of the liquid level from the bottom of the container within a certain time period.

2.3.2. Pressure

The pressure taps are arranged on the test section (Fig. 4a), for the 30 pressure test points to record the pressure at different operating conditions. The pressure data are transmitted via pressure sensor of model 1210 (ICSensor CO.) into voltage and acquired by the data acquisition boards which connected to a computer. The gauge pressures at the total pipes of gas and liquid inlets were read by pressure gauges. The environmental pressure is measured by a mercury barometer.

2.3.3. Temperature

The temperature of the gas and liquid are measured by Dial-type of WSS-4 thermometers which are installed on the pipelines in front of the test section with an overall accuracy of ± 0.2%. The dry and wet temperature of local environment can be read by the dry and wet thermometer with a resolution of 0.5 °C.

3. Data reduction

3.1. Flow ratio

In the presentation of the results for the two-phase distribution measurements, the flow ratio in the ith channel is presented in a normalized manner (Fei, 2003; Marchitto et al., 2008; Vist and Pettersen, 2004):

$$\text{flow ratio} = m_{j,i} = \frac{\dot{m}_{j,i}}{\sum_{i=1}^{n} \dot{m}_{j,i}/10} \tag{1}$$

where $j = G$ (Gas), or $j = L$ (Liquid). The non-dimensional gas flow ratio $m_{G,i}$ is the ratio of the measured mass gas flow rate of ith-channel to the average gas flow rate of the 10 channels. The value of $m_{j,i}$ reflects the uniformity of the liquid and gas phase distribution in different channels.

Two indicators for the overall performance of the non-uniformity of distribution are adopted. One is the maximum difference in $\dot{m}_{j,i}$, called maximum flow maldistribution, denoted by MFM and determined as follows:

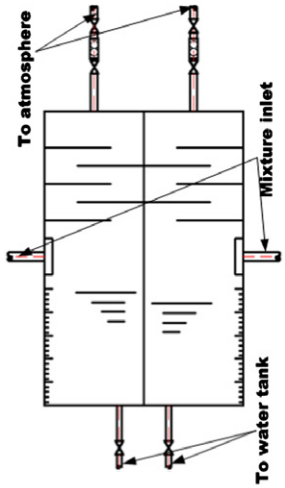

(a) Schematic of the separator

(b) Photo of the separator

Fig. 6. Air–water separator.

$$\mathrm{MFM} = m_{j,\max} - m_{j,\min} \tag{2}$$

The other indicator, which may be more generally, is the root of mean square (RMS) of $\dot{m}_{j,i}$ for all the channels. The RMS denotes the deviation degree of each channel and synthetically represents the maldistribution of the gas or liquid phase in each channel at different experimental operation conditions, which is defined as follows:

$$\mathrm{RMS}_j = \left[\frac{1}{10}\sum_{i=1}^{10}(\dot{m}_{j,i} - 1)^2\right]^{0.5} \tag{3}$$

It can be easily seen that the smaller the MFM, and the smaller the RMS, the more uniform the flow distribution.

3.2. Experimental uncertainty analysis for flow rate

In this study the most important parameter is the flow rate. Its test range and accuracy of measurements are shown in Table 1. The measurement uncertainties are estimated by the procedure described by Kline and McClintock (1953) and Moffat (1988).

In our experiment, as mentioned above, 10 transparent separators were used to separate gas and liquid and for the determination of liquid volume flow rate. A stopwatch was used to record the operating time, during which the liquid height variation h in every separator was recorded. For each channel its volume flow rate of liquid phase can be calculated as follows:

Table 1
Test range and accuracy of the instruments.

Instrument	Range	Accuracy (%)
Rotor volume flow meter for gas outlet	1.67E−03–1.67E−02 $m^3\,s^{-1}$	2.5
Rotor volume flow meter for liquid gross inlet	0–1.11E−03 $m^3\,s^{-1}$	2.5
Pressure gauge for gas gross inlet	0–1 atm	1.6
Pressure gauge for liquid gross inlet	0–600 kPa	1.6
Pressure transducer for test section	0–100 kPa	1.6
Temperature gauge for gas gross inlet	0–100 °C	0.2
Dry and wet temperature	−10 to 100 °C	

$$\overset{*}{Q}_L = \frac{Ah}{\tau} \tag{4}$$

where A is the cross section area of the separator, and τ is the time duration for accumulation of water column with height of h.

The minimum h is 100 mm and the resolution of the reading scale is one millimeter. Considering that some waviness often

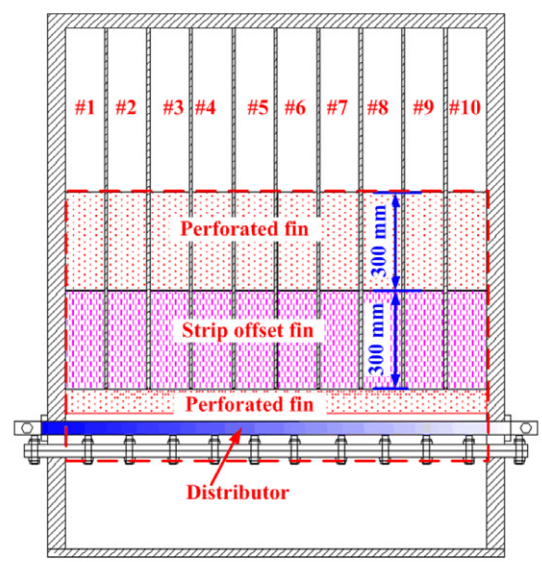

(a) Schematic of the distributor with fins for test section

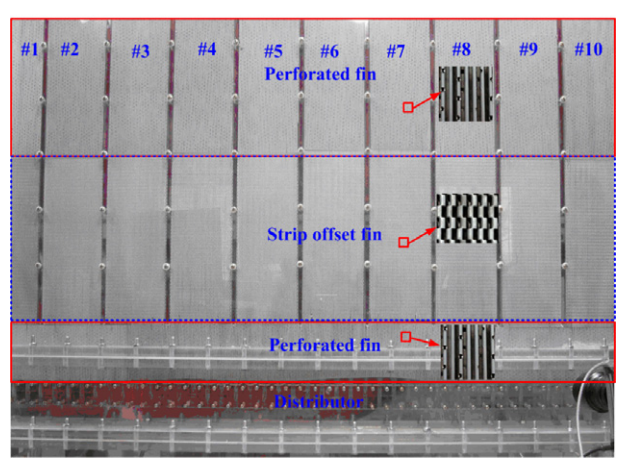

(b) Part of photo for the distributor with fins

Fig. 7. Distributor with aluminum fins.

occurs during the data-taking period, we take 2.0% as the maximum value of the relative uncertainty, i.e., $(\delta h/h)_{\max} = 2.0\%$. It takes no less than 250 s to finish one record of the liquid volume flow ratio, and the resolution of the stopwatch is 0.5 s. Thus we take the maximum uncertainty of time, $(\delta\tau)_{\max}$ equal to 0.5 s. The maximum uncertainty of τ measurement is:

$$\delta\tau/\tau = \frac{0.5}{250} \times 100\% = 0.2\%$$

The uncertainty of $\overset{*}{Q}_L$ is calculated by the following equation:

$$\frac{\delta\overset{*}{Q}_L}{\overset{*}{Q}_L} = \left(\left(\frac{\delta h}{h}\right)^2 + \left(\frac{\delta\tau}{\tau}\right)^2\right)^{0.5} \tag{5}$$

The estimated maximum uncertainty for the liquid volume flow rate is about 2.1%. It should be noted that this measurement uncertainty is estimated by the height of the liquid volume and the related time period, it is not due to the liquid flow unsteadiness.

Table 2
Basically geometry of the fins (unit: mm).

Fin style	Fin spacing	Fin height	Fin thickness	Specification
Strip offset fin	1.4	6.5	0.3	Strip length: 3
Perforated fin	1.4	6.5	0.3	Perforated diameter = 0.5 Opening rate: 10%

4. Results and discussion

The experiment is divided into two parts. First, the fins are not installed after the distributor and ten separated parallel channels are empty and directly connected with the outlet of the distributor part (Fig. 4a); second, two kinds of fins (strip offset fins and perforated fins) are installed in the ten channels, as shown in Fig. 7. Fig. 7a shows the perforated fins in the upper part and the strip offset fins in middle part of the parallel channels in the test section. The fin lengths of these two parts are both 300 mm. In the lower part of the fin region perforated fin of 50 mm is located. Fig. 7b presents the enlarged photographs of the offset fins and perforated fins. The geometries of strip offset fin and perforated fin are listed in Table 2.

4.1. The channels without fins

During the experimental process, the liquid phase volume flow rate is fixed at 1.4E−04, 2.4E−04, 3.7E−04, 4.4E−04, 5.6E−04, 6.1E−04, 6.5E−04 $m^3\,s^{-1}$, respectively and the gas phase volume for rate is adjusted within a certain range for every liquid flow rate. For each test condition data were taken 5 times, and then the averaged one is used for data reduction. The Reynolds numbers for gas and liquid at the gas and liquid inlets of the distributor are from 6.2E+03 to 2.3E+04 and 5.2E+03 to 2.5E+04, respectively. These Reynolds number ranges are taken from the two-phase refrigerants flow in a real brazed plate-fin heat exchanger.

Gas and liquid flow ratios of the 10 parallel channels at the liquid volume flow rate of 1.4E−04 $m^3\,s^{-1}$ and 2.4E−04 $m^3\,s^{-1}$ are

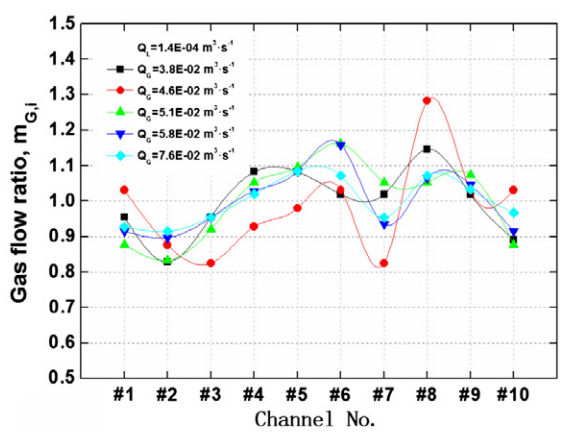

(a) Gas flow ratio vs. channel

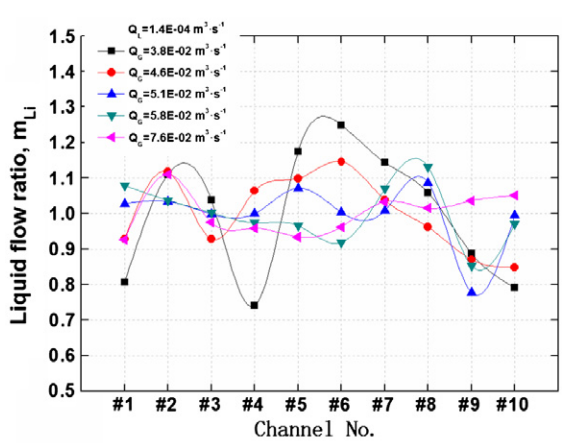

(b) Liquid flow ratio vs. channel

Fig. 8. Gas and liquid flow ratio at Q_L = 1.4E−04 $m^3\,s^{-1}$.

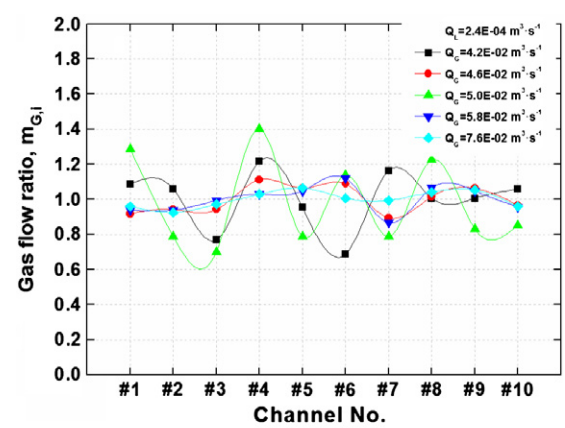

(a) Gas flow ratio vs. channel number

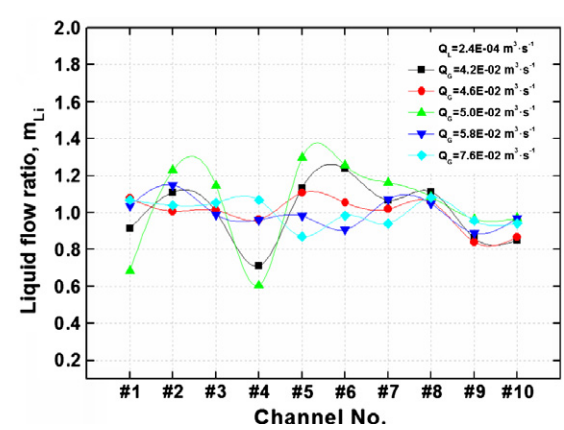

(b) Liquid flow ratio vs. channel number

Fig. 9. Gas and liquid flow ratio at Q_L = 2.4E−04 $m^3\,s^{-1}$.

shown in Figs. 8 and 9, respectively. The results for the liquid volume flow rate of 3.7E−04, 4.4E−04, 5.6E−04, 6.1E−04 and 6.5E−04 $m^3 s^{-1}$ are qualitatively the same. In order to save space, they are not presented in the paper.

When the liquid volume flow rate is in 1.4E−04 $m^3 s^{-1}$, the maximum gas and liquid flow ratios are 1.3 and 1.24, respectively (see Fig. 8a and b); the minimum gas and liquid channel flow ratios are 0.82 and 0.79, respectively. The gas flow ratios (Fig. 8a) of channels 2 and 3 are basically under the average level (=1), and those of channel 6, 8 and 9 are higher than the average level. The flow maldistribution is the most severe for liquid when the gas flow rate is of 3.8E−02 $m^3 s^{-1}$ (Fig. 8b). The liquid channel flow distribution is relative uniform in the other four conditions.

The channel flow ratios for the liquid volume flow rate of 2.4E−04 $m^3 s^{-1}$ are presented in Fig. 9. The maximum gas and liquid flow ratios are 1.40 and 1.25 respectively, and the minimum gas and liquid flow ratios are 0.68 and 0.61, respectively. For this liquid flow rate, the gas and liquid channel flow ratios are the most non-uniform when the gas flow rate is 5.0E−02 $m^3 s^{-1}$.

Generally speaking the gas and liquid flow ratio of the most channels are in the range of 0.8–1.2 for the two liquid volume flow rates. The maldistribution of the distributor studied is less severe than those reported in (Ha et al., 2006; Marchitto et al., 2009; Vist and Pettersen, 2004; Webb and Chung, 2005).

Figs. 10–12 presents the maximum flow maldistribution (MFM) and root of mean square of the flow ratio (RMS) at the six liquid

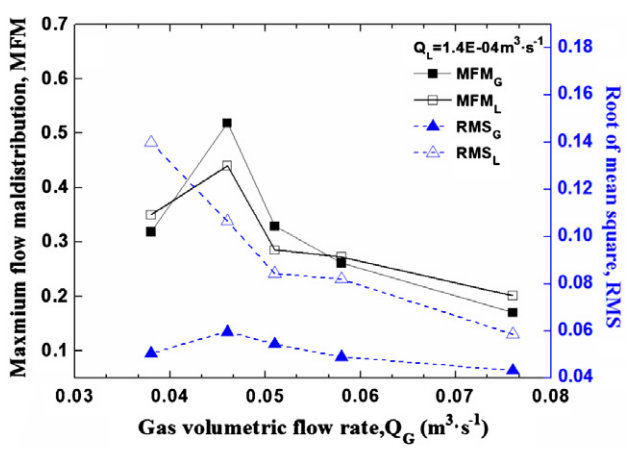

(a) Q_L=1.4E-04 $m^3 \cdot s^{-1}$

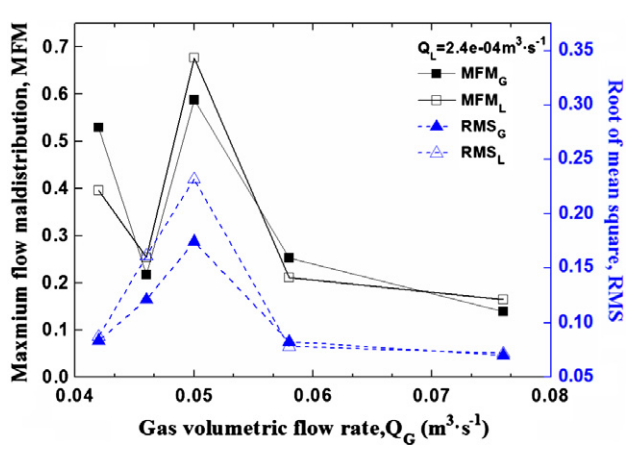

(b) Q_L=2.4E-04 $m^3 \cdot s^{-1}$

Fig. 10. Effects of the gas volume flow rate on the MFM and RMS at Q_L = 1.4E−04 and 2.4E−04 $m^3 s^{-1}$.

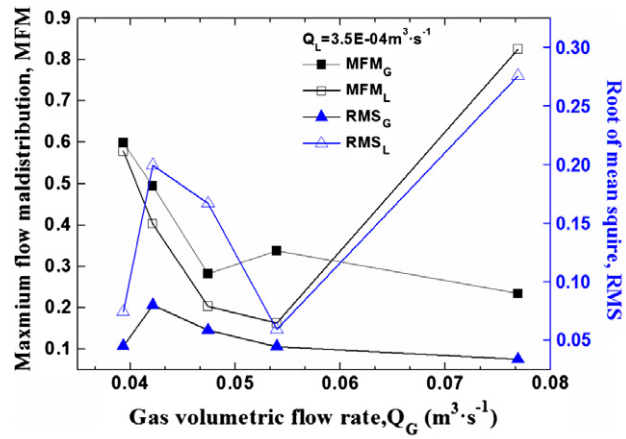

(a) Q_L=3.5E-04 $m^3 \cdot s^{-1}$

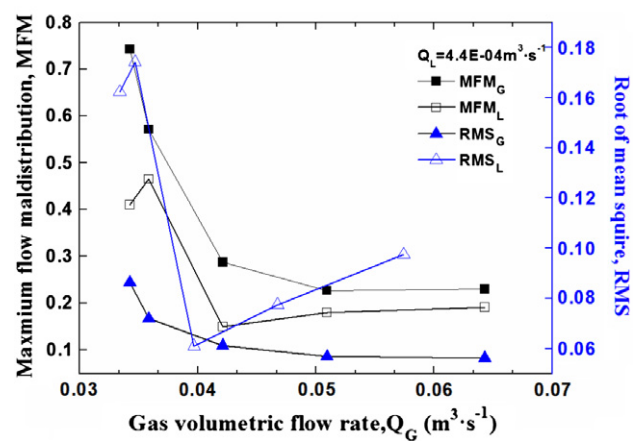

(b) Q_L=4.4E-04 $m^3 \cdot s^{-1}$

Fig. 11. Effects of the gas volume flow rate on the MFM and RMS at Q_L = 3.5E−04 and 4.4E−04 $m^3 s^{-1}$.

flow rates studied with gas flow rate as a parameter. Each indicator has liquid part and gas part represented by the subscript L or G. The maximum flow maldistribution for gas is 0.82 (Fig. 12b). The gas maximum RMS is 0.29 (Fig. 11a). For liquid, the maximum MFM (Fig. 12a) and (Fig. 12b) are both 0.82.

Fig. 10a shows that the maximum flow ratios of gas and liquid are similar and comparable. However, the curve of the gas RMS is below the liquid one, which shows that the gas flow is more uniform than the liquid flow for the five gas flow rates. Also the results of RMS in Figs. 10b, 11 and 12 show the same feature as that in Fig. 10a, i.e., the MFM of liquid is always larger than that of gas.

From Figs. 9 to 12, a general variation trend of the flow maldistribution with the gas flow rate may be observed: in the lower range of gas flow rate, the liquid maldistribution is more severe than that at the high gas flow rate. In our measurement process through visual observation it was found that at the lower gas flow rate the flow pattern of the two-phase flow is more likely to be in the slug flow regime. And the more severe maldistribution at lower gas flow rate may be attributed to this flow pattern.

4.2. The channels with fins

For this test, the liquid phase volume flow rate is fixed at 1.3E−04, 1.7E−04, 2.2E−04, 2.8E−04, 3.3E−04, 3.9E−04, 5.0E−04 and 5.6E−04 $m^3 s^{-1}$, respectively, and the gas phase volume flow rate is changed. Fig. 13 shows the gas and liquid flow rate in 10

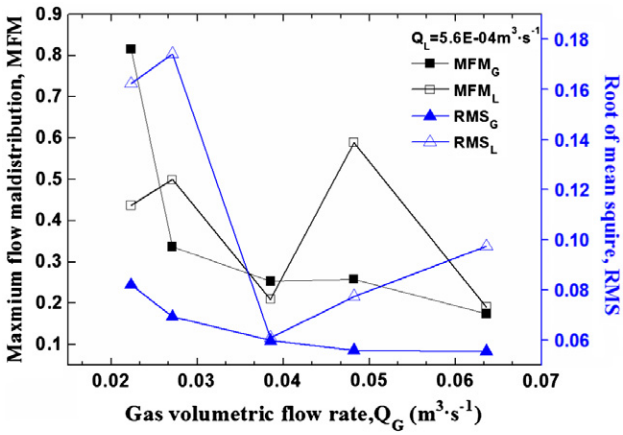

(a) Q_L=5.6E-04 $m^3 \cdot s^{-1}$

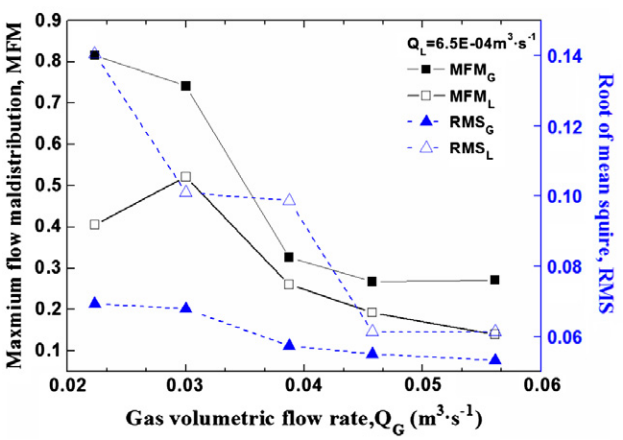

(b) Q_L=6.5E-04 $m^3 \cdot s^{-1}$

Fig. 12. Effects of the gas volume flow rate on the MFM and RMS at Q_L = 5.6E−04 and 6.5E−04 $m^3\ s^{-1}$.

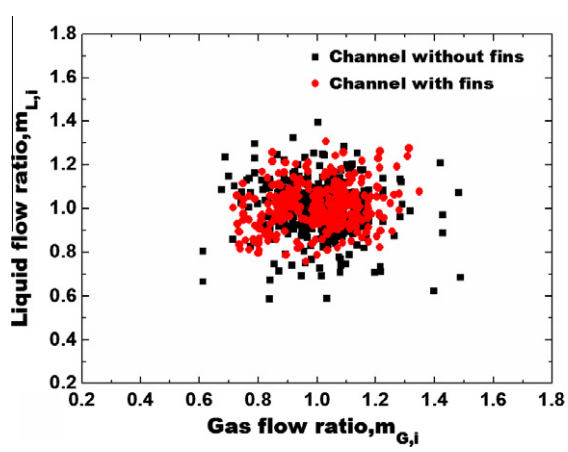

Fig. 13. Gas flow ratio vs. liquid flow ratio of the channel with fins.

parallel channels for all the operating conditions. Gas and liquid flow ratios for the channel without fin are also shown in Fig. 13 for comparison. The liquid and gas flow ratios in 10 parallel channels are mostly in the range of 0.8–1.2 for the channel with fins. Compared the results of channel with and without fins, it can be seen that the channels with fins have more uniform flow distribution than that without fins.

5. Discussion

In this section, comparison is made for the two-phase flow distribution characteristics of two distributors, i.e, the present structure and the flute distributor presented in Marchitto et al. (2009). The air and water distributions occurring in cylindrical horizontal header with 16 parallel vertical channels were investigated for upward flow in their work. Air and water firstly mixed in a long inlet tube outside the header, and then the two-phase mixture was distributed to the parallel channels through a co-axial, multi-hole flute type distributor inserted in the header. The major difference between the above-mentioned distributor of Marchitto et al. and the present work is that in the present work the preliminary mixing of gas and liquid and the distribution of two-phase flow are both finished in the distributor, while in the flute-type distributor the preliminary mixing of gas and liquid is implemented in the long inlet tube, not in the flute-type distributor. It is interesting to note that the separated inlets of gas and liquid in the proposed distributor do not require an additional facility. In a conventional two-phase refrigerating system ahead of the plate-fin heat exchanger there is a tank to store the two-phase refrigerant where gas and liquid phases are separated because of the gravity effect.

The gas and liquid phase flow ratios and their RMS are shown in Fig. 14. It should be noted that: the RMS represents a synthetic index of gas /liquid flow rate maldistribution, and the parameter was previously utilized by Ben Saad et al. (2011) and Marchitto et al. (2008, 2009) for an analysis of multiphase flow maldistribution where the flow patterns of different authors were different. Fig. 14a illustrates the liquid flow ratio against the gas flow ratio

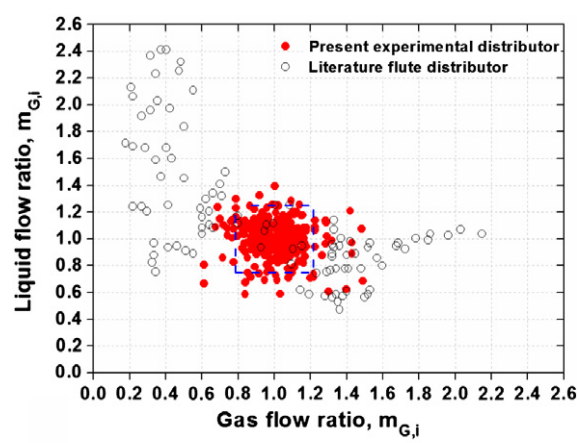

(a) Gas flow ratio vs. liquid flow ratio

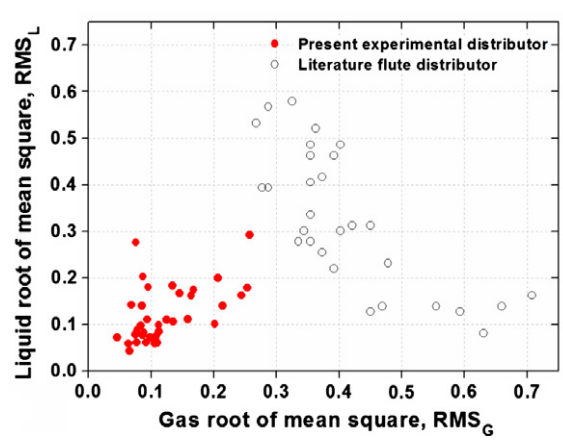

(b) Gas root mean square vs. liquid root mean square

Fig. 14. Comparisons with (Marchitto et al., 2009).

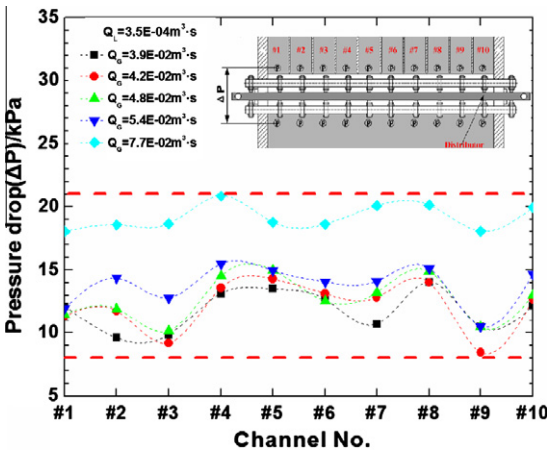

Fig. 15. Pressure drop at $Q_L = 3.5E{-}04\ m^3\ s^{-1}$.

in 10 parallel channels for all the experimental operating conditions (with and without fins) of this study, and the data of flute 180°distributor from Marchitto et al. (2009). The liquid and gas flow ratios for parallel channels mostly lies between the scopes of 0.8–1.2, in other word, the flow maldistribution is within ±20%; while the results for the flute 180°distributor show that gas flow ratio is in the range of 0.2–2.2, and liquid is in the range of 0.5–2.3. As indicated above a good distributor should have gas and liquid flow ratios close to 1. The maximum gas flow ratio for the channels in the present experiment and flute 180°distributor is 1.44 and 2.2, respectively, the minimum gas flow ratio in the present experiment and literature is 0.58 and 0.20, respectively.

From Fig. 14b, the gas and liquid root mean square for gas is in the range of 0.04–0.25, and for liquid is in the range of 0.05–0.29; For the flute 180°distributor (Marchitto et al., 2009), the RMS values for gas is in the range of 0.26–0.7 and for liquid is in the range of 0.08–0.57. As described above the smaller the RMS value the better the distribution. Both the flow ratio and the RMS show that the present structure has a more uniform distribution than that of the flute 180°distributor.

Fig. 15 shows the pressure drop along the distributor zone. The pressure drop (Δp) is 7–21 kPa. Since we did not measure the pressure drop of conventional distributors, no accurate comparison can be made. According to the authors experience there may be several kPa increase in the pressure drop. The improvement in the heat transfer because of the better uniformity of flow distribution can compensate such pressure drop penalty. Hence this new type distributor has been adopted in the plate-fin heat exchanger produced recently in China.

6. Conclusion

In the present study a new style two-phase flow distributor is proposed. The major feature of the proposed distributor is: the two phases flow into the plate-fin heat exchanger separately and then mix each other in the distributor. The two-phase mixture is then supplied to the subsequent channel in one unit. Such distributor is adopted in each unit of the same plate-fin heat exchanger. Following conclusions can be made:

1. For a fixed liquid flow rate there is a gas flow rate at which the two-phase flow distribution becomes worse, and this may be attributed to the occur of slug flow in the parallel channels.
2. In the flow rate range studied, the gas and liquid flow ratios are usually in the rage of 0.8–1.2, indicating a maldistribution of ±20%.
3. The maximum liquid flow ratios of the ten parallel channels are always larger than that of gas.
4. The two-phase flow distribution of the parallel channels with fin is more uniform than that without fins.
5. Comparison with flute 180°distributor the proposed structure has a better flow distribution performance.

Acknowledgment

This work was supported by NNSFC (51136004, U0934005).

References

Ahmad, M., Berthoud, G., Mercier, P., 2009. General characteristics of two-phase flow distribution in a compact heat exchanger. IJHMT 52, 442–450.
Bejan, A., 1997. Constructal-theory network of conducting paths for cooling a heat generating volume. IJHMT 40, 799–816.
Bejan, A., 2000. Shape and Structure, From Engineering to Nature. Cambridge University Press, Cambridge, United Kingdom.
Bejan, A., Tondeur, D., 1998. Equipartition, optimal allocation, and the constructal approach to predicting organization in nature. Rev. Gen. Therm. 37, 165–180.
Ben Saad, S., Clement, P., Gentric, C., Fourmigue, J.F., Leclerc, J.P., 2011. Experimental distribution of phases and pressure drop in a two-phase offset strip fin type compact heat exchanger. Int. J. Multiphase Flow 37, 576–584.
Bernoux, P., Mercier, P., Lebouche, M., 2001. Two-phase flow distribution in a compact heat exchanger. Compact Heat Exchangers and Enhancement Technology for the Process Industries-2001, 347–352,576.
Fei, P., 2003. Adiabatic Developing Two-phase Refrigerant Flow in Manifolds of Heat Exchangers. University of Illinois, Urbana Champaign.
Ha, M.Y., Kim, C.H., Jung, Y.W., Heo, S.G., 2006. Two-phase flow analysis in multi-channel. J. Mech. Sci. Technol. 20, 840–848.
Jiao, A., Baek, S., 2005. Effects of distributor configuration on flow maldistribution in plate-fin heat exchangers. HTrEn 26, 19–25.
Kim, N.H., Han, S.P., 2008. Distribution of air–water annular flow in a header of a parallel flow heat exchanger. IJHMT 51, 977–992.
Kitto, J., Robertson, J.M., 1989. Effects of maldistribution of flow on heat transfer equipment performance. HTrEn 10, 18–25.
Kline, S.J., McClintock, F.A., 1953. Describing uncertainties in single-sample experiments. MecEn 75, 3–8.
Lahey, R., 1986. Current understanding of phase separation mechanisms in branching conduits. NuEnD 95, 145–161.
Lalot, S., Florent, P., Lang, S.K., Bergles, A.E., 1999. Flow maldistribution in heat exchangers. Appl. Therm. Eng. 19, 847–863.
Marchitto, A., Devia, F., Fossa, M., Guglielmini, G., Schenone, C., 2008. Experiments on two-phase flow distribution inside parallel channels of compact heat exchangers. Int. J. Multiphase Flow 34, 128–144.
Marchitto, A., Fossa, M., Guglielmini, G., 2009. Distribution of air–water mixtures in parallel vertical channels as an effect of the header geometry. Exp. Therm. Fluid Sci., 895–902.
Moffat, R.J., 1988. Describing the uncertainties in experimental results. Exp. Therm Fluid Sci. 1, 3–17.
Mueller, A.C., Chiou, J.P., 1988. Review of various types of flow maldistribution in heat exchangers. HTrEn 9, 36–50.
Osakabe, M., Hamada, T., Horiki, S., 1999. Water flow distribution in horizontal header contaminated with bubbles. Int. J. Multiphase Flow 25, 827–840.
Seeger, W., Reimann, J., Muller, U., 1986. Two-phase flow in a T-junction with a horizontal inlet. I: Phase separation. Int. J. Multiphase Flow 12, 575–585.
Tondeur, D., Luo, L.G., 2004. Design and scaling laws of ramified fluid distributors by the constructal approach. ChEnS 59, 1799–1813.
Vist, S., Pettersen, J., 2004. Two-phase flow distribution in compact heat exchanger manifolds. Exp. Therm Fluid Sci. 28, 209–215.
Webb, R.L., Chung, K., 2005. Two-phase flow distribution to tubes of parallel flow air-cooled heat exchangers. HTrEn 26, 3–18.
Wen, J., Li, Y.Z., 2004. Study of flow distribution and its improvement on the header of plate-fin heat exchanger. Cryo 44, 823–831.
Yuan, P., 2003. Effect of inlet flow maldistribution on the thermal performance of a three-fluid crossflow heat exchanger. IJHMT 46, 3777–3787.
Yue, J., Boichot, R., Luo, L.G., Gonthier, Y., Chen, G.W., Yuan, Q., 2010. Flow distribution and mass transfer in a parallel microchannel contactor integrated with constructal distributors. AIChE 56, 298–317.
Zhang, Z., Li, Y.Z., 2003. CFD simulation on inlet configuration of plate-fin heat exchangers. Cryo 43, 673–678.